

SANDIA REPORT

SAND87-8950
Unlimited Release
Printed February 1988

RS-8232-2/66778

Cy2



8232-2/066778



00000002 -

Rutherford Backscattering and Auger Spectroscopy of Mercuric Iodide Detectors

(To be published in Journal of Nuclear Materials)

T. E. Felter, R. H. Stulen, W. F. Schnepple, C. Ortale, L. van den Berg

Prepared by
Sandia National Laboratories
Albuquerque, New Mexico 87185 and Livermore, California 94550
for the United States Department of Energy
under Contract DE-AC04-76DP00789

Issued by Sandia National Laboratories, operated for the United States Department of Energy by Sandia Corporation.

NOTICE: This report was prepared as an account of work sponsored by an agency of the United States Government. Neither the United States Government nor any agency thereof, nor any of their employees, nor any of the contractors, subcontractors, or their employees, makes any warranty, express or implied, or assumes any legal liability or responsibility for the accuracy, completeness, or usefulness of any information, apparatus, product, or process disclosed, or represents that its use would not infringe privately owned rights. Reference herein to any specific commercial product, process, or service by trade name, trademark, manufacturer, or otherwise, does not necessarily constitute or imply its endorsement, recommendation, or favoring by the United States Government, any agency thereof or any of their contractors or subcontractors. The views and opinions expressed herein do not necessarily state or reflect those of the United States Government, any agency thereof or any of their contractors or subcontractors.

SAND87-8950
Unlimited Release
Printed February 1988

Rutherford Backscattering and Auger Spectroscopy of Mercuric Iodide Detectors

T. E. Felter and R. H. Stulen
Sandia National Laboratories, Livermore, CA 94550

and

W. F. Schnepple, C. Ortale and L. van den Berg
EG&G, Inc. Santa Barbara Operations, Goleta CA 93117

Abstract

Palladium contacts on mercuric iodide have been studied using Rutherford Backscattering Spectroscopy and Auger Electron Spectroscopy. Results on actual detector contacts show some intermixing of both mercury and iodine with the palladium. To investigate the role of processing variables as a possible cause of this effect we have fabricated "model contacts" at low temperatures ($T \approx 100$ K) and analyzed *in situ*. The results demonstrated that significant interdiffusion occurs at temperatures as low as 225 K. We conclude that excessive heating during contact deposition could prove to be detrimental to device performance and that the use of cooled substrates during processing should be explored.

Interest in mercuric iodide as a room temperature x-ray detector has increased rapidly over the last few years. Crystals are now grown larger and with greater purity than ever before. However, to make a detector, or any other electrical device, it is necessary to form high quality electrical contacts to the crystal. At present, the deposition and formation of contacts is both poorly understood and irreproducible among the different laboratories engaged in detector fabrication. For example, EG&G has found gold to be a very poor contact material for HgI_2 presumably because of readily formed compounds of gold, mercury and iodine. On the other hand, Tadjine et. al. [1] have formed stable contacts with gold. Similar discrepancies are found for other surface related effects, for example, Nicolau [2] has found HNO_3 to be a useful electrochemical etchant prior to contact deposition but that a KI solution worked poorly. Precisely the opposite results were obtained by EG&G which now uses a standard KI chemical etch based process for cutting and polishing prior to evaporation of contacts.

The present work represents the first experimental study using modern surface science techniques to investigate the metal-insulator interface between the contact and the mercuric iodide crystal. Both Rutherford Backscattering Spectroscopy (RBS) and Auger Electron Spectroscopy (AES) have been used in these studies. In all cases reported here, the contact material was palladium, which has generally been the most successful choice. The contacts investigated included ones fabricated at Sandia by the same techniques used to make actual working detectors, as well as ones fabricated in an ultra high vacuum chamber on a HgI_2 substrate cooled to low temperature to avoid sublimation. These latter contacts are termed "model contacts" since they were produced in a manner slightly different than for production detectors. The utility of these model contacts is that they can be readily analyzed by Auger electron spectroscopy *in situ* during fabrication at temperatures where interdiffusional effects and chemical reaction rates between the metal and the HgI_2 are minimized. Measurements on actual detector contacts were made with both RBS and AES.

Rutherford Backscattering Spectroscopy (RBS)

RBS was performed with 2 MeV $^4\text{He}^+$ particles at a backscattering angle of 150° on specimens which were inserted into the vacuum chamber after Pd contacts were evaporated onto the mercuric iodide crystals in a separate deposition system. For the deposition process, the polished HgI_2 crystals are inserted into a diffusion pumped bell jar where the Pd is deposited by evaporation from a hot tungsten filament. The total time between the insertion into and removal from the deposition chamber was less than 10 min. (the actual evaporation step took place in less than one minute). RBS spectra were obtained for the sample at room temperature, the Pd contact serving as a barrier to sublimation of the underlying HgI_2 crystal during the course of the measurements. The barrier is desirable both from the standpoint of reducing contamination to the vacuum chamber and of losing sample material from the surface region which could lead to stoichiometry changes.

The energy of the backscattered $^4\text{He}^+$ particles is measured with a silicon surface barrier detector and depends on two things: the mass of the target atom that produces the turn around event and the total path length of the $^4\text{He}^+$ ion in the solid. Since the particle loses energy due to electronic excitation as it traverses the sample, the particles exhibiting the greatest energy loss represent those that penetrated deepest into the sample. The recoil energy of the backscattered ions depends on the target mass according to simple classical ideas of scattering; thus, the heavier target particles give rise to higher energy backscattered particles [3].

Figure 1 shows the RBS spectrum from an "as received" detector fabricated at room temperature. The leading step in the spectrum, at approximately 1.8 MeV, is due to ions backscattered from mercury atoms at the Pd/ HgI_2 interface. Since mercury is the heaviest atom of the target, ions backscattered from it are highest in energy, even though some energy is lost in traversing the evaporated Pd film. The next feature in the spectrum, a step at approximately 1.72 MeV, is due to backscattering from two different regions: iodine at the contact interface and palladium at the free surface. Iodine, being lighter than mercury, produces a lower energy backscattered $^4\text{He}^+$. Palladium, being lighter still, would have its

edge appear at even lower energy except that the incident ions can scatter directly off its surface without traversing the metal film. In the present experiment, these two regions are not resolved. At still lower energy in the spectrum, at 1.68 MeV, a downward going step can be seen. This feature is due to palladium at the contact interface region. No evidence of impurities was found in these measurements, but it should be borne in mind that RBS is not very sensitive to the most likely contaminants, carbon and oxygen.

Figure 1 also contains the results of model calculations of RBS using the RUMP code [4]. Two examples are shown differing only in the assumption of the thickness of the Pd contact, 200 and 500 Å. The two simulations nicely bracket the experimental curve. The relative heights of the steps indicate that the stoichiometry is close to that of HgI₂. The calculation includes broadening based on measurement of the instrument resolution. Some additional broadening is apparent which suggests that the contact may not be perfectly uniform in thickness. Moreover, both steps in the experiment have tails which extend to higher energy than the calculations. This suggests some interdiffusion of the mercuric iodide towards, and possibly onto the Pd surface.

Auger Electron Spectroscopy (AES)

We have also studied the Pd/HgI₂ interface using Auger electron spectroscopy [5]. The surface sensitivity of this technique greatly exceeds that of RBS because of the short escape depth of the Auger electrons ($< 10\text{Å}$). Two types of specimens were investigated: those fabricated as described in the RBS section, above (i.e. actual detector contacts), and those on model contacts grown *in situ* in the UHV chamber. For the former, specimens were inserted into the UHV system (base pressure 1×10^{-10} Torr) through a rapid sample insertion stage onto a liquid nitrogen cooled assembly. Transfer and cool down times were on the order of 10 minutes or less. Once the sample was cooled to $T < 150\text{ K}$, the AES spectra were taken using a 3-keV primary electron beam and a double pass CMA spectrometer (PHI model 15-255G).

"Model contacts" were produced *in situ* by first depositing a thin layer ($< \sim 5000\text{ Å}$) of HgI₂ from a room temperature capsule containing HgI₂ which was inserted into the UHV system to within $\sim 1\text{ cm}$ of a cold ($T \approx 100\text{ K}$) sapphire

substrate mounted on a small heater assembly. The sapphire had a thin palladium contact which had previously been evaporated onto it in the bell jar. Growth of the HgI_2 film could be monitored by observing the development of interference fringes as the layer thickness increased. After HgI_2 deposition, Pd could be evaporated *in situ* using a small tungsten wire source. A chromel alumel thermocouple was mounted directly onto the sapphire to monitor temperature changes during evaporation and for later annealing treatments. A temperature increase of less than 5 K was typically observed during Pd deposition.

On all detector contacts fabricated using a standard Pd deposition process onto room temperature HgI_2 crystals, significant, in some cases as much as one monolayer, quantities of both mercury and iodine were found on the surface of the palladium contact. Figure 2 shows an example of an Auger spectrum for an "as received" detector contact fabricated at room temperature. The contact covers the entire free surface of the HgI_2 crystal, approximately 1 cm^2 . The electron beam is focussed to approximately 1 mm^2 . In addition to Pd, both Hg and I are seen on the surface of the contact. This suggested to us that interdiffusion of the mercuric iodide and the palladium may have occurred during the deposition at room temperature and that a more detailed examination of the kinetics during interface formation would be very beneficial. To this end we developed techniques described above to deposit both HgI_2 and Pd onto a liquid nitrogen cooled substrate in the UHV system.

For thick layers of mercuric iodide grown at substrate temperatures of less than 150 K, Auger spectroscopy showed that the surface stoichiometry was close to that of HgI_2 . However, warming the sample to 260 K caused significant changes in the surface composition, a decrease in the iodine signal and an increase in the Hg signal were observed in the AES spectra indicating a change in stoichiometry in the direction of mercurous iodide. Any studies of the kinetics associated with the interface between the metallic contact and the mercuric iodide must therefore necessarily be done at temperatures below 260 K.

To examine interdiffusional effects we have constructed layered sandwich structures of Pd/ HgI_2 /Pd on top of sapphire, where the mercuric iodide layer was less than $\sim 1 \text{ }\mu\text{m}$ thick (based on the number of interference fringes

observed during growth). The outermost Pd layer was less than or equal to approximately 500 Å (still transparent but with a slight metallic sheen evident visually). These structures which were initially grown at $T \sim 100$ K were then isochronally annealed (5 min.) at successively higher temperatures, cooled back to 100 K and examined with AES. After depositing the Pd film, only palladium was visible in the Auger spectra. Figure 3 shows the Auger signal (peak-to-peak height) for iodine and mercury after various annealing treatments. Two types of regions on the sample were examined: regions which had not yet been exposed to the primary AES beam (3 keV), designated "virgin" areas, and those which had seen the electron beam previously, designated "damaged" areas. Measurements of the sample temperature during the AES indicated temperature rises of less than 2 K. The excellent thermal conductivity of the substrate and the thinness of the film insures that the temperature of the sample in the region of the incident electron beam is not appreciably raised.

The top two curves in the figure are for the virgin regions and have been shifted upward to avoid overlap with the bottom two curves. It is clear that the iodine and mercury track one another for both sets of curves. For annealing treatments below 175 K both I and Hg are essentially zero and cannot be distinguished from the noise in the AES spectra. At 200 K, however, the virgin regions exhibit appreciable iodine and mercury signals, with further increases occurring after the 275 K anneal. The final anneal to room temperature was for only 2 minutes, but nevertheless exhibits some further increases. Overall, the behavior shown for the damaged regions is similar except for the fact that the onset for the iodine and mercury signals is shifted to slightly higher temperatures. Thus, the beam damage appears to "fix" the interface somewhat, it delays the interdiffusion to a higher temperature. Note that this is in the opposite direction as would occur, for example, by beam heating effects since for that case the temperature of the sample in the area of the incident electron beam would be higher than the temperature measured by the thermocouple. An alternate explanation is that the primary beam may desorb the I and Hg through electron-stimulated desorption.

A second example of sequential heating of a Pd/HgI₂/Pd sandwich structure is shown in figure 4. In this case, the data were all taken on damaged regions and more annealing cycles were obtained in order to follow the kinetic process in

more detail. The same general trends are observed: a rapid increase in iodine and mercury levels is seen at and above the 225-K annealing temperature. For the data shown in this figure, all of the annealing treatments were for 5 minutes.

Summary

It is clear from both the RBS and AES results presented here that palladium contacts on HgI_2 cannot be viewed as an undisturbed metallic film resting on top of a perfect mercuric iodide crystal. From these studies we can identify at least two phenomena that may affect the stoichiometry of the contact interface region and which therefore may affect the electrical properties of the contact. The first of these is the preferential loss of iodine from the surface upon vacuum exposure. This implies that during vacuum deposition processes, a thin layer of mercurous iodide may form prior to or during Pd evaporation depending on the temperature of the crystal and the length of time it remains under vacuum prior to evaporation. Secondly, above 200 - 225 K there is significant intermixing of Pd with the substrate crystal. If this interpenetration becomes severe, the metallic nature of the contact will be lost causing failure of the device (we have observed this effect for Cu contacts on HgI_2). Both of these effects indicate that one should take care to prevent excessive heating of the sample during contact deposition. We suggest that processing techniques explore the use of cooled substrates during contact deposition. Sputter deposition should also be explored especially since this technique is less likely to raise the temperature of the substrate in a production environment.

The effects presented here could also be important in the degradation of detectors over long periods of time. Certainly, prevention of storage at elevated temperatures should avoid long term degradation and enhance the survivability.

We would like to acknowledge helpful conversations with R. James and the technical assistance of Glenda Gentry, Steve Haney, and Dan Morse. This work was supported by the U. S. Department of Energy under contract DE-AC04-76DP00789.

References

- [1] A. Tadjine, J. M. Koebel, M. Amann, and P. Siffert, published in these proceedings; and private communication.
- [2] Y. F. Nicolau and P. Moser, published in these proceedings; and private communication.
- [3] see for example: Ion Beam Handbook for Material Analysis , Edited by: J. W. Mayer and E. Rimini, (Academic Press 1977).
- [4] developed by L. Doolittle at Cornell University.
- [5] see for example: Photoelectron and Auger Spectroscopy ,T. A. Carlson (Plenum, 1975).

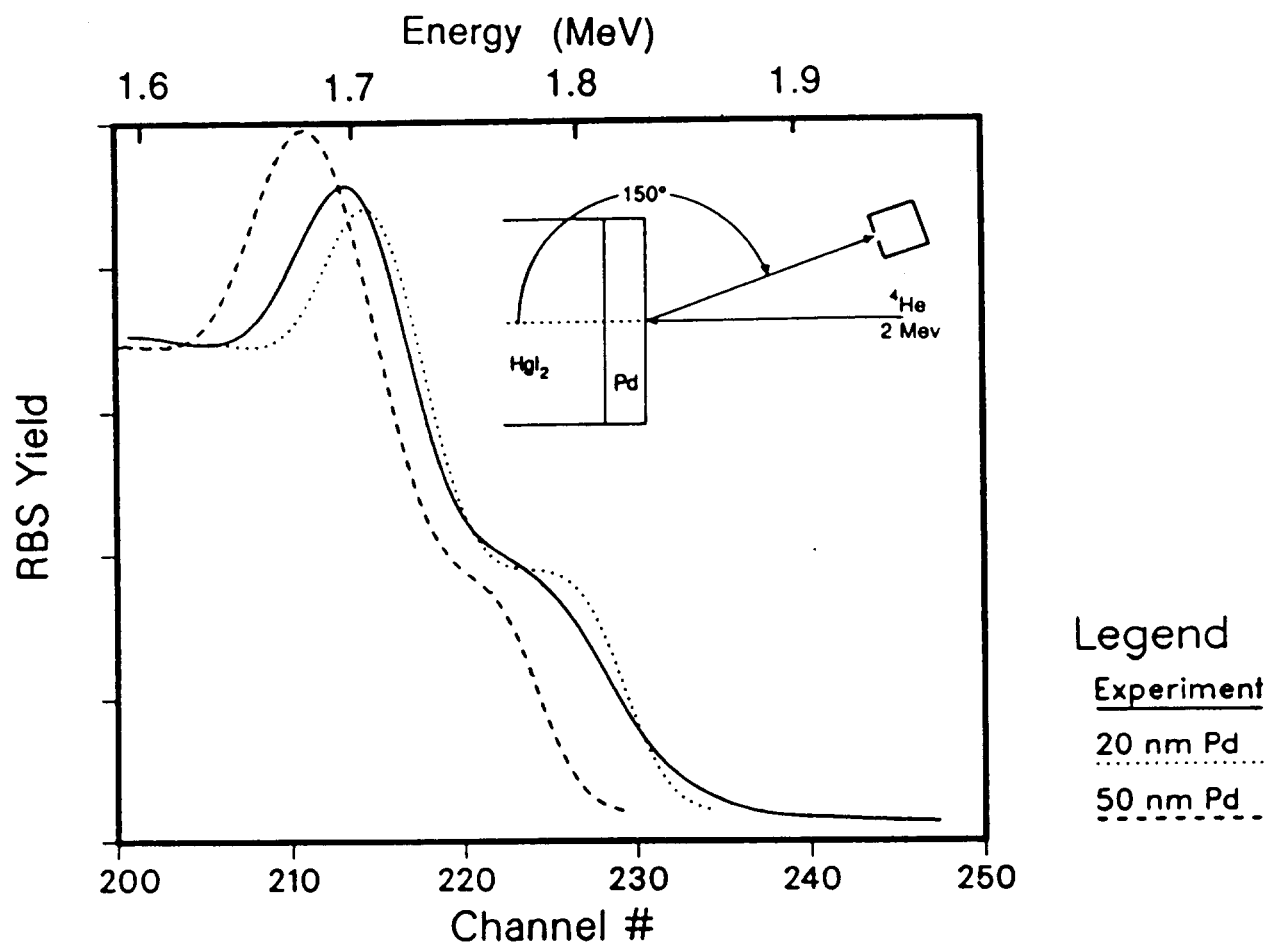


Figure 1. 2 MeV Rutherford Backscattering Spectrum of an "as received" Pd contact on a mercuric iodide detector. Also shown are two computer simulations which bracket the experimental spectrum.

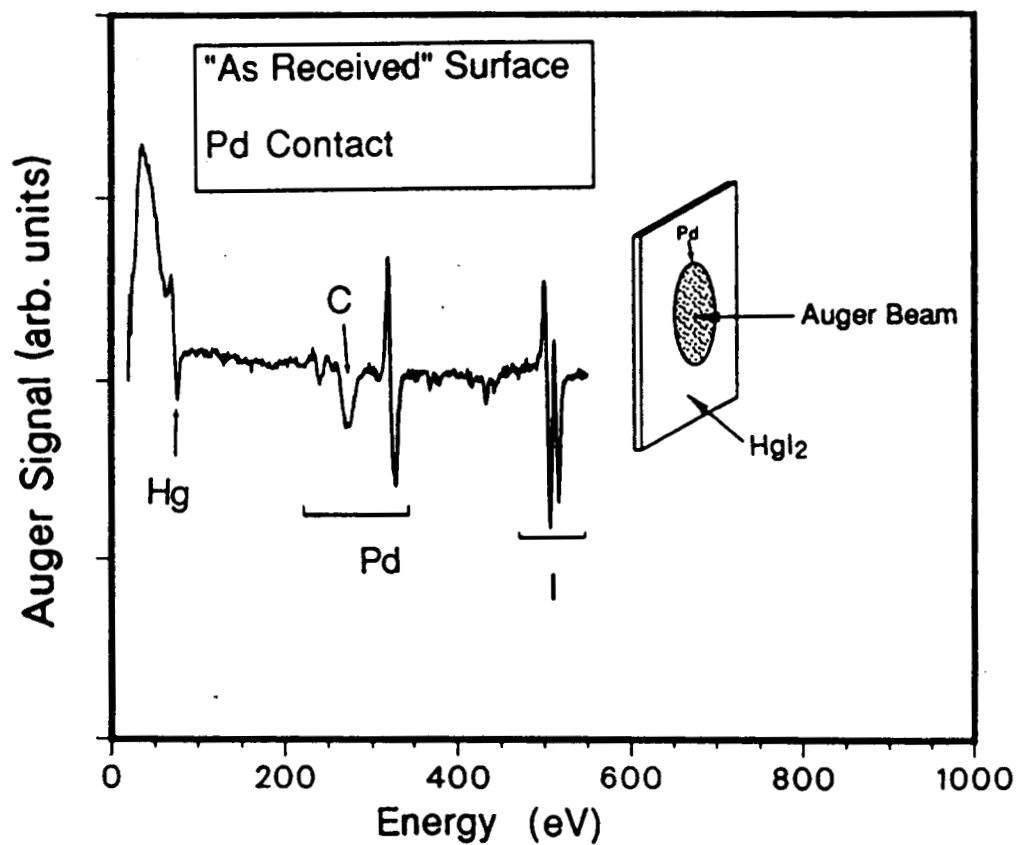


Figure 2. Auger spectrum of an "as received" Pd contact on a mercuric iodide detector showing the existence of mercury and iodine on top of the contact. The contact covers the entire crystal surface (approximately 1 cm²) and the Auger beam samples a small portion of it (approximately 1 mm²).

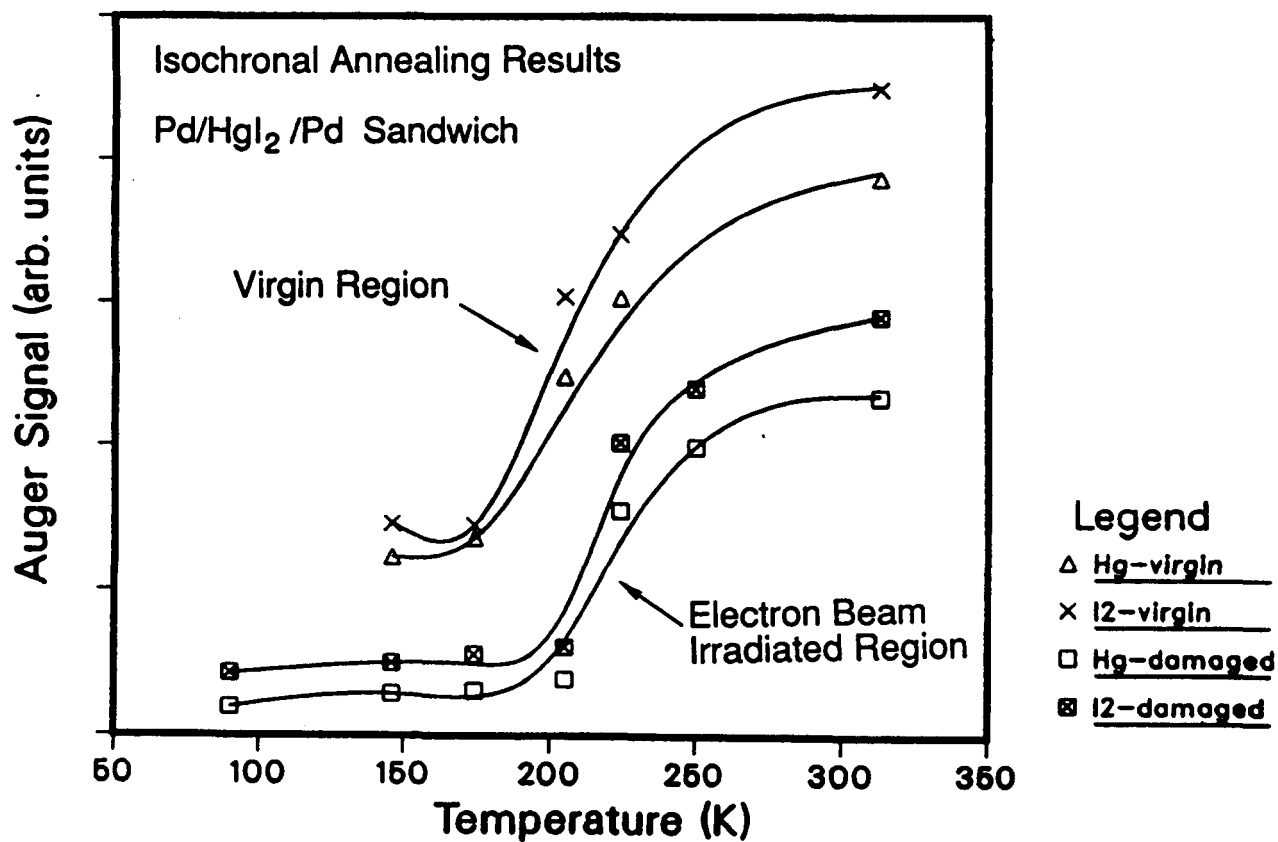


Figure 3. Annealing sequence for a Pd/HgI₂/Pd sandwich structure. Except for the 2 minute anneal at 300 K, all the anneals were performed for a duration of 5 minutes. Two types of regions were investigated, those which had never previously seen the electron beam (shifted upward in the figure) and those which had previously seen the electron beam.

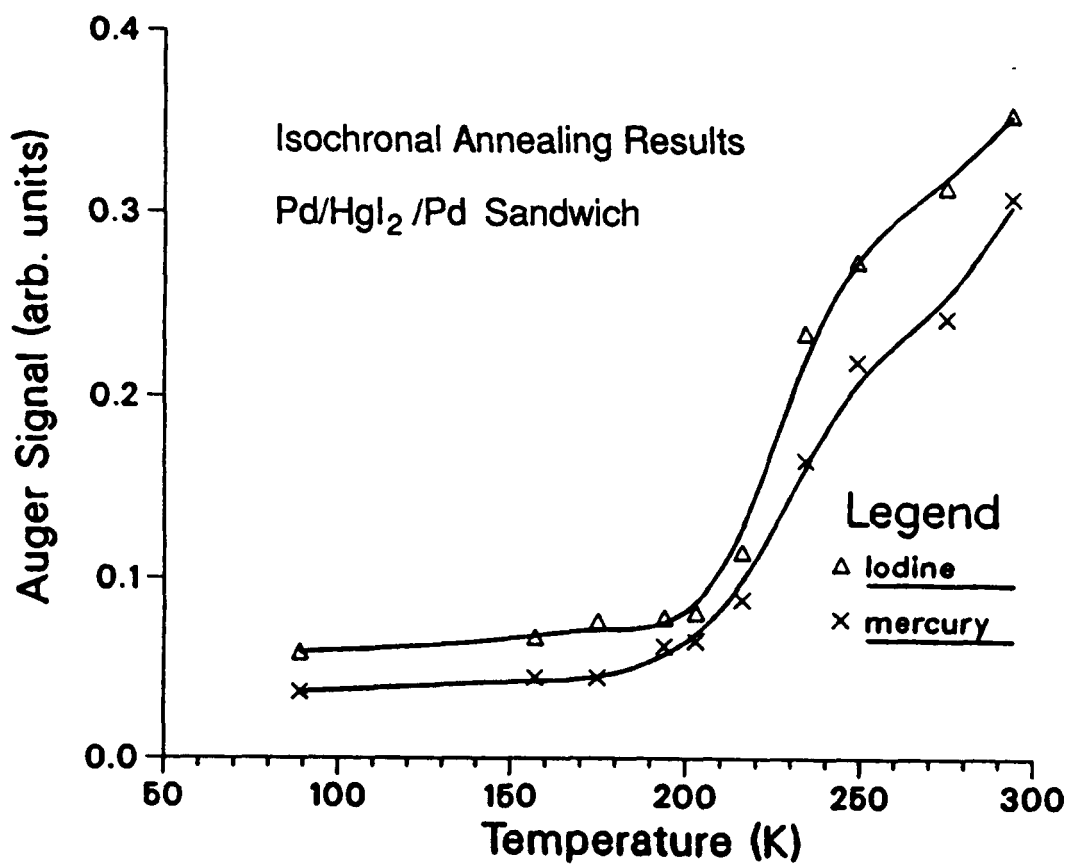


Figure 4. Similar to figure 3 except all anneals performed for 5 minutes and only regions of the sample that had see the electron beam are plotted. The sequence has more annealing cycles so as to display the kinetics more completely.

UNLIMITED RELEASE
INITIAL DISTRIBUTION

Abteilung C1
Hahn-Meitner Institut
Attn: J. R. Schneider
Glienickerstr. 100
D-1000 Berlin 39
F. R. G.

Albert-Ludwigs-Universität
Kristallographisches Inst.
Attn: M. Grün
Helberstr. 25
7800 Freiburg
F. R. G.

Albert-Ludwigs-Universität
Kristallographisches Inst.
Attn: H. Marquardt
Helberstr. 25
7800 Freiburg
F. R. G.

Albert-Ludwigs-Universität
Kristallographisches Inst.
Attn: K. Wacker
Helberstr. 25
7800 Freiburg
F. R. G.

AFIF
ETH Hönggerberg
Attn: S. Blunier
8093 Zürich
Switzerland

AFIF
ETH Hönggerberg
Attn: H. Zogg
8093 Zürich
Switzerland

Aristot. Univ. Thessaloniki
Physics Department
Attn: E. K. Polychroniadis
54006 Thessaloniki
Greece

Carnegie Mellon University
Dept. of Elec. & Computer Eng.
Attn: T. E. Schlesinger
Pittsburgh, PA 15213

Contraves
Attn: H. Stanna
Schaffhauserstr. 580
8052 Zürich
Switzerland

EG&G Measurements Inc.
Santa Barbara Operations
Attn: A. Beyerle
130 Robin Hill Road
Goleta, CA 93117

EG&G Measurements Inc.
Santa Barbara Operations
Attn: A. Y. Cheng
130 Robin Hill Road
Goleta, CA 93117

EG&G Measurements Inc.
Santa Barbara Operations
Attn: L. A. Franks
130 Robin Hill Road
Goleta, CA 93117

EG&G Measurements Inc.
Santa Barbara Operations
Attn: V. M. Gerrish
130 Robin Hill Road
Goleta, CA 93117

EG&G Measurements Inc.
Santa Barbara Operations
Attn: H. A. Lamonds
130 Robin Hill Road
Goleta, CA 93117

EG&G Measurements Inc.
Santa Barbara Operations
Attn: J. M. Markakis
130 Robin Hill Road
Goleta, CA 93117

EG&G Measurements Inc.
Santa Barbara Operations
Attn: C. Ortale
130 Robin Hill Road
Goleta, CA 93117

EG&G Measurements Inc.
Santa Barbara Operations
Attn: B. E. Patt
130 Robin Hill Road
Goleta, CA 93117

EG&G Measurements Inc.
Santa Barbara Operations
Attn: M. Schieber
130 Robin Hill Road
Goleta, CA 93117

EG&G Measurements Inc.
Santa Barbara Operations
Attn: W. F. Schnepple
130 Robin Hill Road
Goleta, CA 93117

EG&G Measurements Inc.
Santa Barbara Operations
Attn: N. Skinner
130 Robin Hill Road
Goleta, CA 93117

EG&G Measurements Inc.
Santa Barbara Operations
Attn: L. van den Berg
130 Robin Hill Road
Goleta, CA 93117

ESA
Microgravity Office
Attn: G. Seibert, Prog. Mgr.
8-10, Rue Mario-Nikis
75738 Paris, Cedex 15
France

ESA
Microgravity Office
Attn: H. Walter, Senior Scientist
8-10, Rue Mario-Nikis
75738 Paris, Cedex 15
France

Fachbereich Physik
Universität Siegen
Attn: H.-J. Besch
Adolf-Reichweinstr.
5900 Siegen 21
F. R. G.

Ferroperm Ltd.
Electronic Components
Attn: P. Lindhardt
Stubbeled 7, Trorod
2950 Vedbaek
Denmark

Fisk University
Dept. of Physics
Attn: E. Silberman
Nashville, TN 37203

Global Geochemistry Corp
Attn: S. Steinberg
6919 Eton Avenue
Canoga Park, CA 91303

The Graduate School, Nagatsuta
Tokyo Inst. Technology
Attn: T. Kobayashi
Midori-ku, Yokohama 227
Japan

Inst. Angewandte Physik
Universität Karlsruhe
Attn: U. Birkholz
Kaisestr. 12
D-7500 Karlsruhe
F. R. G.

Inst. Mittelenergiephysik
ETH Hönggerberg
Attn: J. Lang
8093 Zürich
Switzerland

IRDI
Dept. Electron. Instr. Nucl.
Attn: A. Friant
C.E.N. Saclay
91191 Gif-sur Yvette, Cedex
France

IRDI

Dept. Electron. Instr. Nucl.
Attn: J. Mellet
C.E.N. Saclay
91191 Gif sur Yvette, Cedex
France

Institut für Physik
Universität Basel
Attn: I. Zschokke-Gränacher
Klingerbergstr. 82
4056 Basel
Switzerland

Inst. TESRE/CNR
Attn: G. Di Cocco
Via de Castagnoli 1
40126 Bologna
Italy

Inst. TESRE/CNR
Attn: W. Dusi
Via Castagnoli 1
40126 Bologna
Italy

Inst. TESRE/CNR
Attn: C. Labanti
Via Castagnoli 1
40126 Bologna
Italy

Instrum. Appl. Phys. Div.
Harwell
Attn: D. Tottendell
Oxfordshire OX11 0RA
England

Jap. Atomic Energy Res. Inst.
Attn: E. Sakai
Tokaimura Nakagun
Ibarakiken 319-11
Japan

Jet Propulsion Laboratory
California Inst. of Technology
Attn: J. G. Bradley
4800 Oak Grove Drive
Pasadena, Ca 92209

Jet Propulsion Laboratory
California Inst. of Technology
Attn: J. M. Conley
4800 Oak Grove Drive
Pasadena, Ca 92209

Jet Propulsion Laboratory
California Inst. of Technology
Attn: P. L. Schlichta
4800 Oak Grove Drive, 11-116
Pasadena, Ca 91109

Kristal-Mater. Labor.
Fak. Physik, Univ. Karlsruhe
Attn: G. Müller-Vogt
Kaiserstr. 12
7500 Karlsruhe 1
F. R. G.

Lab. Chimie Minerale 1
U.E.R. Sciences Exactes Nat.
Attn: J. Omaly
B. P. 45
63170 Aubière
France

Lab. Mineral-Cristallogr.
Attn: S. Léon-Gits
Tour 16, 4 Place Jussieu
75320 Paris, Cedex
France

Labor. für Festkörperphysik
ETH Hönggerberg
Attn: G. Busch
8093 Zürich
Switzerland

Labor. Festkörperphysic
ETH Hönggerberg
Attn: E. Kaldis
8093 Zurich
Switzerland

Labor. Festkörperphysik
ETH Honggerberg
Attn: M. Piechotka
8093 Zürich
Switzerland

Labor. Festkörperphysik
ETH Hönggerberg
Attn: P. Wachter
8093 Zürich
Switzerland

Laboratoire PHASE
C. R. N.
Attn: B. Biglari
B. P. 20
F-67037 Strasbourg-Cedex
France

Laboratoire PHASE
C. R. N.
Attn: M. Hage-Ali
B. P. 20
60737 Strasbourg Cedex
France

Laboratoire PHASE
C. R. N.
Attn: J. M. Koebel
67037 Strasbourg, Cedex
France

Laboratoire PHASE
C. R. N.
Attn: M. Samimi
B. P. 2
67037 Strasbourg Cedex
France

Laboratoire PHASE
C. R. N.
Attn: P. Siffert
67037 Strasbourg, Cedex
France

Laboratoire PHASE
C. R. N.
Attn: A. Tadjine
B. P. 20
67037 Strasbourg, Cedex
France

LETI/CRM
CEA-CENG, 85X
Attn: M. Cuzin
38041 Grenoble, Cedex
France

LETI/CRM
CEA-CENG, 85X
Attn: Y. F. Nicolau
38041 Grenoble, Cedex
France

Link Analytical Ltd.
Attn: B. Lowe
Halifax Road, High Wycombe
Bucks, England HP12 3SE

Link Analytical Ltd.
Attn: R. Sareen
Halifax Road, High Wycombe
Bucks HP12 3SE
England

LPMC-CNRS
UA 796-UER Sciences
Attn: R. Cadoret
B. P. 45
63170 Aubière
France

Max-Planck Inst. Phys. Astroph.
Institut. für Extratr. Physik
Attn: T. Economou
c/o Dr. D. Hovestadt
8046 Garching bei München
F. R. G.

Metallurgie Hoboken Overpelt
Attn: G. Knockaert
A. Greinerstr. 14
2710 Hoboken
Belgium

NASA Headquarters
Microgravity Sci. & Appl. Div.
Code EM-7
Attn: K. Scholl
Washington, DC 20546

National Bureau of Standards
Attn: B. Steiner
Washington, DC

Office of Naval Research Branch
Division of Administration
Attn: L. Smith
223 Old Marylebone Road
London NW1 5TH
United Kingdom

Osaka University
Dept. Electrical Engineering
Faculty of Engineering
Attn: M. Suita
Osaka 565
Japan

Osaka University
Dept. Electrical Engineering
Faculty of Engineering
Attn: T. Taguchi
Osaka 565
Japan

Philips Forschungslab. GmbH
Attn: H. Scholz
Postfach 1980
D-5100 Aachen
F. R. G.

Phytoresource Research Inc.
Attn: Y. F. Abdeemessih
101E, 707 Texas Ave.
College Station, TX 77840

Radiation Monitoring Devices
Attn: G. Entine
44 Hunt St.
Watertown, MA 02172

Radiation Monitoring Devices
Attn: J. C. Lund
44 Hunt Street
Watertown, MA 02172

Robert Gordons Inst. Physics
School of Physics
Attn: J. Rennie
St. Andrews Street
Aberdeen AB1 1HG
Scotland

Robert Gordons Inst. Physics
School of Physics
Attn: M. A. S. Sweet
St. Andrews Street
Aberdeen AB1 1HG
Scotland

Schlumberger Doll Research
Attn: K.-L. Giboni
Old Quarry Road
Ridgefield, CT 06877

Scientific Industrial Automation P/L
Attn: K. J. Lieber
70 Maryborough St.
Fyshwick, ACT 2609
Australia

Scientific Industrial Automation P/L
Attn: N. F. Robertson
70 Maryborough St.
Fyshwick, ACT 2609
Australia

Scientific Industrial Automation P/L
Attn: N. Shoustov
70 Maryborough St.
Fyshwick, ACT 2609
Australia

Siemens AG Centr. Technol. Div.
Central Res. Develop., Res. Lab.
Attn: P. A. Glasow
Paul-Gossen Str. 100
D-8520 Erlangen
F. R. G.

Siemens AG Centr. Technol. Div.
Central Res. Develop., Res. Lab.
Attn: J. Walter
Paul-Gossen Str. 100
D-8520 Erlangen
F. R. G.

Techn. Büro für Kristallzücht
Auftragforschung u. Gerätebau
Attn: G. Lamprecht
Lehningerstr. 10-12
D-7531 Neuhausen
F. R. G.

Techn. Büro für Kristallzücht.
Auftragforschung u. Gerätebau
Attn: R. Lauck
Lehningerstr. 10-12
D-7531 Neuhausen
F. R. G.

Tohoku Inst. of Technology
Attn: Y. Hirata
35-1, Yagiyama Kasumicho
Sendai 982
Japan

Tohoku Inst. of Technology
Attn: K. Ohba
35-1, Yagiyama Kasumicho
Sendai 982
Japan

Tohoku Inst. of Technology
Attn: T. Shoji
35-1, Yagiyama Kasumicho
Sendai 982
Japan

Tokyo Denshi Yakin Co.
Attn: H. Onabe
1361 Akabane
Chigasaki-City
Kanagawa-Pref.
Japan

Toyama University
Faculty of Engineering
Attn: H. Nakatani
3190 Gofuku
Toyama 930
Japan

University of California
Dept. of Material Science Engineering
Attn: L. Keller
Los Angeles, CA 90024

University of California
Dept. Mater. Sci. Enger.
Attn: R. Ostrom
Los Angeles, CA 90024

University of California
Dept. Mat. Sci. Engineering
Attn: C. M. J. Wagner
Los Angeles, Ca 90024

University of California
Dept. Mech. Environ. Eng.
Attn: F. Milstein
Santa Barbara, CA 93106

University of California
Dept. of Physics
Attn: J. L. Merz
Santa Barbara, CA

Université Louis Pasteur
Lab. Spectr. Opt. Corps Solids
Attn: C. Schwab
5, Rue de l'Université
67084 Strasbourg, Cedex
France

Univ. Missouri-Columbia
Res. Reactor, Dept. Phys.
Attn: W. B. Yelon
Columbia, MO 65211

Univ. Southern California
Inst. Phys. Imaging Sci.
Attn: A. J. Dabrowski
4676 Admiralty Way, Suite 932
Marina del Ray, CA 90291

Univ. Southern California
 Inst. Phys. Imaging Sci.
 Attn: J. S. Iwanczyk
 4676 Admiralty Way, Suite 932
 Marina del Ray, CA 90291

Universität Bonn
 Mineral. Petrogr. Inst. Museum.
 Attn: F. Wollrafen
 Poppelsdorfer Schloss
 D-5300 Bonn
 F. R. G.

Universite de Clermont II
 Attn: B. Coupat
 B. P. 45
 63170 Aubière
 France

Univ. Clermont Ferrant II
 Attn: S. Erraji
 B. P. 45
 63170 Aubière
 France

Universite de Clermont II
 Attn: J. P. Fournier
 B. P. 45
 63170 Aubière
 France

J. H. Ewins, L-278

1000 V. Narayanamurti
 1100 F. L. Vook
 1110 S. T. Picraux
 1112 S. M. Myers
 1113 R. C. Hughes
 1113 S. R. Kurtz
 1113 S. J. Martin
 1140 P. S. Peercy
 1144 D. S. Ginley
 1150 J. E. Schirber
 1800 R. L. Schwoebel
 4030 G. W. Kuswa
 6000 D. L. Hartley

8000 J. C. Crawford
 8100 E. E. Ives
 8200 R. J. Detry
 8300 P. L. Mattern
 8310 R. W. Rohde
 8340 W. Bauer
 8341 M. I. Baskes
 8341 R. B. James
 8341 G. J. Thomas
 8342 M. Lapp
 8343 R. H. Stulen
 8343 T. E. Felter (30)
 8347 K. L. Wilson
 8400 R. C. Wayne
 8500 P. E. Brewer

 9000 R. L. Hagengruber
 9210 H. M. Dumas
 9211 T. G. Taylor
 9220 G. H. Mauth
 9221 J. L. Williams
 9222 L. S. Walker
 9223 D. A. Reynolds
 9224 L. J. Ellis
 9230 R. E. Spalding
 9231 J. C. Chavez
 9232 B. C. Walker
 9233 F. T. Noda
 9234 W. B. Goldrick
 9240 G. E. Brandvold
 9241 R. L. Ewing
 9241 D. J. Mitchell
 9242 R. M. Hall
 9243 P. B. Herrington

8535 Publication Div./ Technical
 Library Processes Div., 3141

3141 Technical Library Processes
 Div. (3)

8524-2 Central Technical Files (3)